Energy Engineering

Tech Science Press

Doi:10.32604/ee.2025.073914

ARTICLE

Research on Coordinated Operation Strategies for Wind Power Hybrid Energy Storage Systems Based on Model Predictive Control

Jiguang Wu[1], Qing Zhi[2,*], Jin Guan[2], Ruopeng Zhang[2], Lixia Wu[2], Shuhui Zhang[2] and Caifeng Wen[3,4]

[1]Inner Mongolia Power (Group) Corporation Limited, Hohhot, 010051, China
[2]Inner Mongolia Power (Group) Corporation Limited—Inner Mongolia Power Research Institute Branch, Hohhot, 010051, China
[3]School of Energy and Power Engineering, Inner Mongolia University of Technology, Hohhot, 010051, China
[4]Inner Mongolia Key Laboratory of Renewable Energy and Energy Storage Technology, Hohhot, 010051, China

*Corresponding Author: Qing Zhi. Email: cjx121382025@163.com

Received: 28 September 2025; Accepted: 21 November 2025; Published: 18 June 2026

ABSTRACT: This paper proposes a hybrid energy storage control method that coordinates the minimum output of the wind–storage system and the SOC self-recovery capability, applied to stand-alone energy storage stations. Under the premise of meeting the wind power smoothing requirements, model predictive control (MPC) is employed to rapidly regulate the SOC and output of the energy storage system during the smoothing process, thereby enhancing its sustained and stable operation capability, and decomposing the original wind power into a direct grid-connected component and a hybrid energy storage smoothing component. Subsequently, the Northern Goshawk Algorithm-Improved Complete Ensemble Empirical Mode Decomposition with Adaptive Noise (NGO-ICEEMDAN) method is employed to decompose and reconstruct the hybrid energy storage power obtained from MPC rolling optimization by determining the optimal combination of white noise amplitude weight Nstd and the number of noise additions (NA), and to allocate the reconstructed power between the supercapacitor and the battery. Finally, simulation verification is conducted using actual 100 MW wind power data from a site in Inner Mongolia. The results demonstrate that the proposed strategy can coordinate the relationship among the minimum output of the hybrid energy storage system (HESS), SOC balancing, and grid-connected power fluctuations. The NGO-ICEEMDAN method enables more precise power allocation, thereby improving the rationality and efficiency of energy management in wind power hybrid energy storage systems.

KEYWORDS: Standalone energy storage power station; hybrid energy storage system; model predictive control; empirical mode decomposition; multi-objective optimization

1 Introduction

Driven by the "dual-carbon" goals, the installed capacity of wind power has been continuously expanding. However, the intermittent and fluctuating nature of wind power output imposes increasingly stringent requirements on the stable operation of power systems [1]. To mitigate wind power fluctuations, wind farms are typically equipped with hybrid energy storage systems, which achieve smooth grid integration through the coordinated operation of energy-type and power-type storage units. In recent years, Model Predictive Control (MPC) [2,3], owing to its multivariable and rolling optimization capabilities, has been widely applied in wind power regulation and grid integration. This approach effectively suppresses power fluctuations while satisfying grid connection constraints [4–6]. Nevertheless, the optimization performance of energy storage

systems largely depends on the accuracy of power decomposition and the determination of the target power profile [7,8].

In existing studies, Variational Mode Decomposition (VMD) and Wavelet Packet Decomposition (WPD) have been widely employed for the multi-scale decomposition of wind power signals to enable optimal configuration of energy storage systems across different time scales [9,10]. International scholars who originally proposed the VMD method, have demonstrated its effectiveness in analyzing wind speed and wind power signals [11]. The method can accurately extract dominant frequency components and thereby facilitate the smoothing control of wind power output. Domestic researchers have further integrated VMD with energy management models to decompose wind power fluctuations and optimize hybrid energy storage power allocation, thereby improving system stability and energy storage utilization [12,13].

Meanwhile, WPD has also been extensively applied in short-term wind power forecasting and smoothing control. Several studies have utilized WPD to extract the high- and low-frequency components of wind power, thereby enhancing the response accuracy of prediction models [14]. Despite these advances, VMD still relies heavily on empirical selection of mode numbers and penalty parameters, resulting in limited adaptability; it is also prone to mode mixing and boundary effects under noisy conditions [15]. Although WPD exhibits excellent time–frequency localization characteristics, its performance is highly sensitive to the decomposition level and the choice of basis functions [16]. This sensitivity can lead to feature energy leakage, high computational complexity, and poor real-time performance, which restrict its applicability in online optimization and control scenarios.

Some scholars have introduced MPC technology for the control of complex multivariable wind power systems. Due to its rolling optimization characteristics, MPC is widely used in power system control to solve multivariable optimal control problems [17]. Reference [18] proposes a two-stage MPC scheme that ensures accurate tracking of wind power fluctuations and achieves precise charge and discharge task decomposition for HESS through rolling optimization at different time scales. Literature [19] aims to minimize energy storage output and maintain charge-discharge balance, optimizing energy storage system performance while meeting grid power constraints. Reference [20] proposes a two-layer MPC method, where the outer layer determines the target power and the inner layer ensures that the actual output power follows the target power through charge and discharge constraints. Additionally, Reference [21] have improved system stability by adjusting the relationship between the state of charge of the energy storage system and grid power fluctuations, using Kalman filters and genetic algorithms to optimize energy storage target power, minimizing energy storage capacity changes and power fluctuations. Reference [22] proposed a hybrid energy storage power allocation strategy based on NGO algorithm-optimized VMD parameters. However, the adaptability and noise handling capability of VMD are far inferior to those of ICEEMDAN.

This study proposes an improved adaptive noise complete ensemble empirical mode decomposition method based on the Northern Goshawk Optimization (NGO) algorithm, termed NGO-ICEEMDAN, for the decomposition of wind power signals. The proposed method optimizes the decomposition parameters to enhance mode separation accuracy and noise robustness, effectively mitigating mode mixing and signal distortion. On this basis, a Model Predictive Control (MPC) strategy with state-of-charge (SOC) self-recovery capability is introduced. Furthermore, a minimum output constraint of the energy storage system is incorporated into the traditional objective function, enabling dynamic determination of the target power for wind power smoothing and coordinated power allocation through rolling optimization. Simulation results based on real wind power data demonstrate that the proposed MPC + NGO-ICEEMDAN approach exhibits superior performance in mitigating grid-connected power fluctuations, coordinating energy storage charge-discharge operations, and improving overall system economy.

2 Model Predictive Control-Based Wind Power Fluctuation Mitigation and Target Power Calculation Model for Energy Storage

Due to the nonlinear, multivariable coupling, multi-constraint, and uncertainty characteristics of wind-storage joint control systems, traditional control methods face challenges in achieving precise modeling, thereby limiting control effectiveness. MPC, with rolling optimization at its core, offers excellent speed and robustness, making it widely applicable in the field of power system control. This section aims to smooth wind power fluctuations while considering the output and lifespan of the energy storage system. By taking the optimal grid-connected power and the minimal output of the hybrid energy storage system as the coupled optimization objectives of the MPC, the rolling optimization method is used to effectively determine the target power for wind power smoothing.

2.1 Structure of Wind-Storage Power Generation System and MPC Predictive Model

The HESS studied in this paper is used to smooth wind power fluctuations, as shown in Fig. 1. The HESS is composed of lithium iron phosphate batteries and supercapacitors, centrally configured on the AC bus, and integrated with wind turbines through power electronic devices to form a wind-storage hybrid system [23]. The power controller of the energy storage system adjusts the output power based on real-time wind power, grid-connected power, SOC of the storage system, and total output of the HESS.

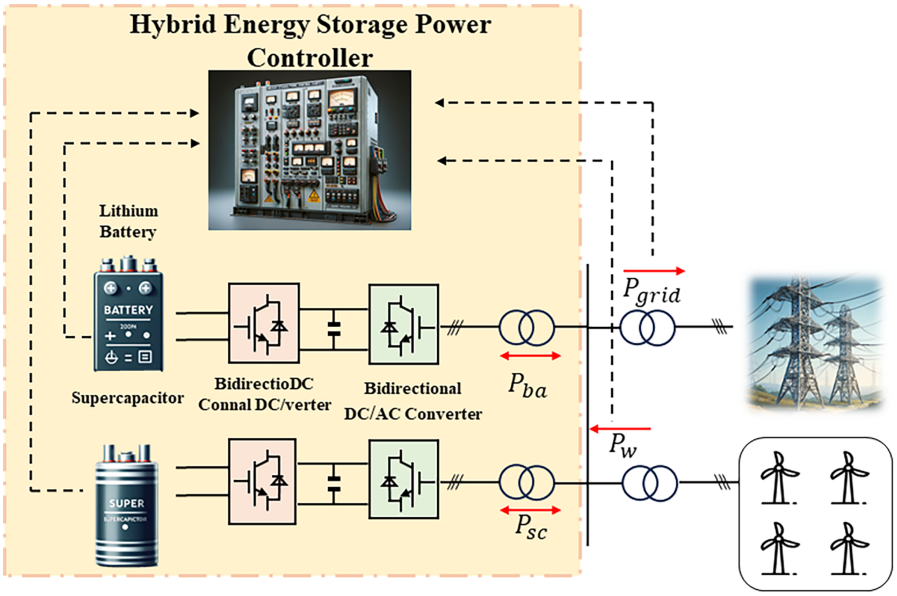

Figure 1: Wind power system structure with HESS

The system employs a single-loop current control strategy for the DC/DC converter and a dual-loop voltage-current control strategy for the DC/AC converter. These strategies effectively mitigate the impact of wind power fluctuations on the hybrid energy storage system, ensuring compliance with grid interconnection technical requirements.

By employing these control strategies, the hybrid energy storage system can effectively suppress the power fluctuations of wind energy, meeting the technical requirements for grid interconnection and enhancing the overall stability and efficiency of the power system.

Based on the power reference directions given in Fig. 1, the following can be shown in Eq. (1).

$$\begin{cases} P_g = P_{es} + P_w \\ P_{ES} = P_{ba} + P_{sc} \end{cases} \tag{1}$$

According to state space theory, assuming the state variable at the current time is $x(k)$, the control input is $u(k)$, the disturbance input is $r(k)$, and the output is $y(k)$, the discrete state space equation of the system can be obtained by discretizing Eq. (2).

$$x(k+1) = Ax(k) + Bu(k) + Cr(k) \tag{2}$$

$$P_g(k+1) = P_{ba}(k) + P_{sc}(k) + P_w(k) \tag{3}$$

In this context, k represents the control time step. As seen from Eq. (3), the grid-connected power of wind power generation, the regulation power of the battery, and the regulation power of the supercapacitor influence each other. Additionally, the output capacity of the energy storage system is affected by its state of charge and discharge. After discretization, the charge and discharge operating states of the battery and the supercapacitor can be described as follows Eq. (4).

$$SOC_{ES}(k+1) = SOC(k) + T_S P_{ES}(k)/Q_{ES} \tag{4}$$

Since the capacity of the HESS is primarily based on the large-capacity battery, the *SOC* of the HESS is considered to be determined by the *SOC* of the battery. Therefore, the process of regulating the *SOC* of the battery will be regarded as the regulation of the *SOC* of the hybrid energy storage system. Combining Eqs. (2)–(4), and assuming the system's state variables $x(k) = [P_g(k), SOC_{ES}(k)]$ control variable $u(k) = P_{ES}(k)$, and disturbance input $r(k) = P_W(k)$, we obtain the MPC predictive model is Eq. (5).

$$\begin{bmatrix} P_g(k+1) \\ SOC_{ES}(k+1) \end{bmatrix} = \begin{bmatrix} 0 & 0 \\ 0 & 1 \end{bmatrix} \begin{bmatrix} P_g(k) \\ SOC_{ES}(k) \end{bmatrix} + \begin{bmatrix} -1 \\ \dfrac{T}{Q_{ES}} \end{bmatrix} [P_{ES}(k)] + \begin{bmatrix} 1 \\ 0 \end{bmatrix} P_w(k) \tag{5}$$

Comparing Eqs. (2) and (5), the coefficient matrices are obtained as Eq. (6).

$$\mathrm{A} = \begin{bmatrix} 0 & 0 \\ 0 & 1 \end{bmatrix}, \mathrm{B} = \begin{bmatrix} -1 \\ \dfrac{T}{Q_{ES}} \end{bmatrix}, \mathrm{C} = \begin{bmatrix} 1 \\ 0 \end{bmatrix} \tag{6}$$

2.2 MPC Optimization Objective Based on Charge-Discharge Saturation Capability Function

Adopting the "charge-discharge saturation capability function $\rho(SOC)$" from reference [23] to quantify the compensation margin between the energy storage unit and wind power fluctuations, the *SOC* of battery is shown in Eq. (7).

$$\rho(SOC) = \begin{cases} 1 - \dfrac{(1-R)e^{I(-SOC+a)}}{1+(1+R)(e^{I(-SOC+a)}-1)} (0 < SOC < 0.5) \\ 1 - \dfrac{(1-R)e^{I(SOC-b)}}{1+(1+R)(e^{I(SOC-b)}-1)} (0.5 < SOC < 1) \end{cases} \tag{7}$$

where R is the initial value of $\rho(SOC)$; a and b are the inflection points of the *SOC*; and I is the parameter representing the variation rate of the control function. The charge and discharge saturation capability curve of the hybrid energy storage system is shown in Fig. 2.

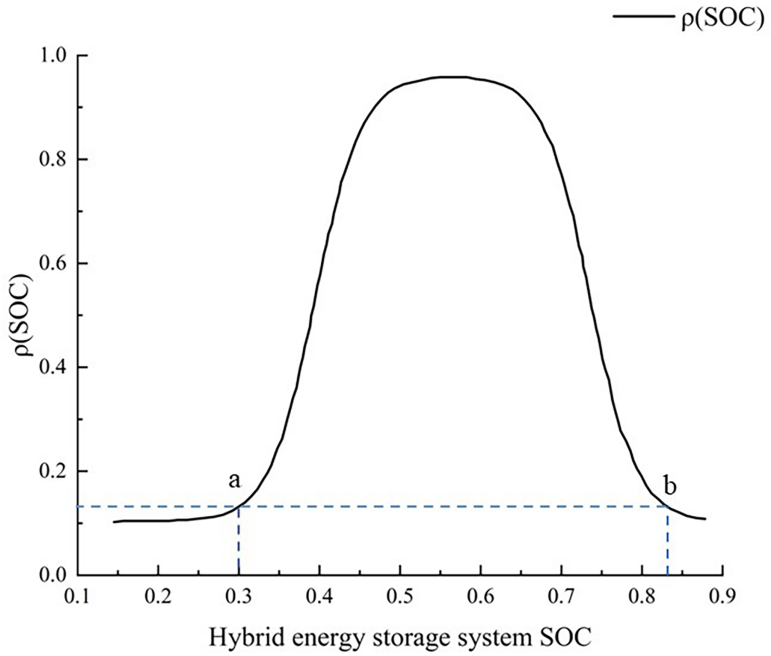

Figure 2: Charge and discharge capability curves of the hybrid energy storage system

As shown in Fig. 2, when the *SOC* is around 0.5, the value of $\rho\,(SOC)$ approaches 1, indicating that the HESS has a good charge and discharge margin at this point. When the *SOC* is less than a or greater than *b*, $\rho\,(SOC)$ exhibits an inflection point and rapidly approaches 0. When the *SOC* is close to 0.1 or 0.9, the HESS also loses its charge and discharge capability.

This paper comprehensively considers the relationship among the grid-connected power fluctuation rate of the wind farm, the minimum output of the energy storage system, and the *SOC* balance of the system. Combining the minimum output of the energy storage system with the *SOC* self-recovery method, the target function is obtained through the coupling relationship among these three factors are shown in Eq. (8).

$$J = \min\{c*(1-\rho\,(\mathrm{SOC}))(\sum_{i=0}^{n}(SOC_{ES}\,(k+i)-0.5)^2 + d*(1-\rho\,(\mathrm{SOC}))\sum_{i=0}^{n}P_{ES}\,(k+1)^2) + (\rho\,(\mathrm{SOC}))\sum_{i=0}^{n}\left(\Delta P_g\,(k+i-1)\right)^2\} \tag{8}$$

In the equation, *c* and *d* represent the weights of the energy storage system output and the system *SOC* balance, respectively, and $c + d = 1$. When $c > d$, the system prioritizes maintaining a stable *SOC* operation; conversely, when $d > c$, the focus shifts towards minimizing the energy storage system's output to reduce the usage of the energy storage system while meeting grid power requirements. Expressed as $\Delta P_g = P_g(k) - P_g(k-1)$. n represents the prediction time length.

The optimization objective function in Eq. (8) includes three parts: adjusting the *SOC* state of the energy storage system, controlling the output of the energy storage system, and adjusting the fluctuation rate of the grid-connected power. By changing the weight coefficients, i.e., the charge-discharge saturation capability function $\rho\,(SOC)$, dynamic adjustment of the three objectives is achieved.

The constraints corresponding to the optimization objective function of the wind-storage system are obtained as Eqs. (9)–(11).

$$-P_{\max} \le P_{ES}(k+1) \le P_{\max} \tag{9}$$

$$SOC_{ES\min} \le SOC_{ES}(k+i) \le SOC_{ES\max} \tag{10}$$

$$\frac{\left|P_g(k) - P_g(k-1)\right|}{P_{rate}} \le \delta \tag{11}$$

2.3 Solving for Energy Storage Power Based on MPC Rolling Optimization

Based on the principles of MPC, and combining Eqs. (2) and (7) along with constraints Eqs. (9)–(11), the problem can be transformed into a quadratic programming (QP) form for solution to obtain the target power for smoothing by the hybrid energy storage system. $x(k)$ is the observable state at time k. According to Eq. (2), the state variable at time $k+1$, $x(k+1)$, can be obtained, and then the state variable at time $k+2$ can be calculated as Eq. (12).

$$x(k+2) = A^2x(k) + ABu(k) + ACr(k) + Bu(k) + BCr(k) \tag{12}$$

Based on the function $x(k)$, the state variable expression at each time step can be derived, consisting of known state variables, disturbance inputs, and control variables to be determined. Assuming the state variable sequence, control variable sequence, and disturbance input sequence are respectively denoted as $X(k)$, $U(k)$, $R(k)$, the expressions are as Eq. (13).

$$X_k = \begin{bmatrix} x(k+1) \\ x(k+2) \\ \cdots \\ x(k+N) \end{bmatrix} U(k) = \begin{bmatrix} u(k+1) \\ u(k+2) \\ \cdots \\ u(k+N) \end{bmatrix} R(k) = \begin{bmatrix} r(k+1) \\ r(k+2) \\ \cdots \\ r(k+N) \end{bmatrix} \tag{13}$$

Let $x(k) = x_0$, then Eq. (2) can be expanded as Eq. (14), the specific expressions can be represented as Eqs. (15)–(17).

$$X_k = Gx_0 + IU_k + MR_k \tag{14}$$

$$G = \begin{bmatrix} A \\ A^2 \\ \cdots \\ A^3 \end{bmatrix} \tag{15}$$

$$I = \begin{bmatrix} B & 0 & \cdots & 0 \\ AB & B & \cdots & 0 \\ \cdots & \cdots & \cdots & \cdots \\ A^{p-1}B & A^{p-2}B & \cdots & B \end{bmatrix} \tag{16}$$

$$M = \begin{bmatrix} C & 0 & \cdots & 0 \\ AC & C & \cdots & 0 \\ \cdots & \cdots & \cdots & \cdots \\ A^{p-1}C & A^{p-2}C & \cdots & C \end{bmatrix} \tag{17}$$

Transform the objective function into a standard quadratic programming form through the above matrix operations is Eq. (18).

$$\min J = \frac{1}{2} U_k^T H U_k + U_k^T f \tag{18}$$

This paper uses the Fmincon function to solve the above MPC optimization problem. The rolling optimization process is as follows: at each time step k, the optimal hybrid energy storage target power is predicted based on the current state and information, but only the first control variable in the sequence is applied to the system. As the system progresses to the next time step $k + 1$, the prediction sequence is updated based on new state information, and optimization is performed again. By continuously updating and correcting, the errors introduced by model inaccuracies and external disturbances can be reduced, thereby improving control accuracy throughout the entire control process.

3 Hybrid Energy Storage Power Allocation

3.1 Power Allocation Framework for HESS

As shown in Fig. 3, the target power calculated by the MPC for the HESS can preliminarily meet the needs of smoothing wind power fluctuations. To fully utilize the advantages of lithium batteries and supercapacitors in the HESS, it is necessary to finely coordinate the target power distribution to achieve efficient operation and long-term stability of the system. Throughout the process, the characteristics of the batteries and supercapacitors should be fully leveraged: batteries should be used to smooth large power variations, while supercapacitors should handle high-frequency power fluctuations to extend the lifespan of the batteries. This paper proposes the NGO-ICEEMDAN method to optimize the power distribution strategy for the hybrid energy storage system.

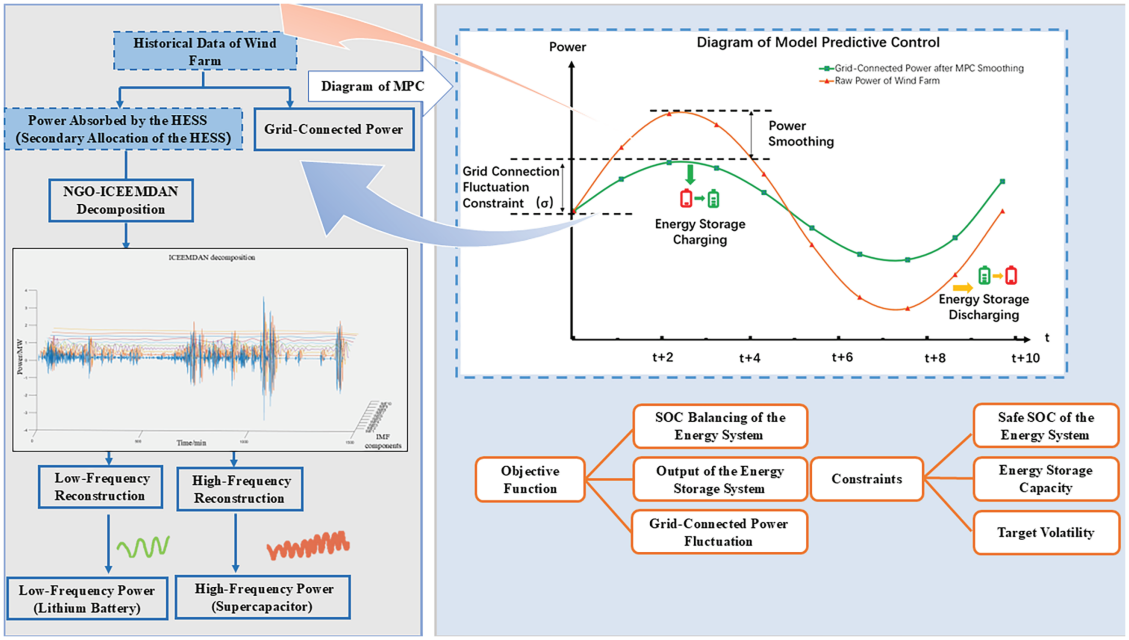

Figure 3: Power distribution frame diagram of hybrid energy storage system

3.2 Power Allocation Based on the ICEEMDAN Method

Wind power is characterized by nonlinear variations and instability, necessitating the use of nonlinear decomposition methods. These power variations include a variety of complex dynamic behaviors that conventional linear methods cannot fully capture. Therefore, nonlinear decomposition methods, such as Empirical Mode Decomposition (EMD) or its improved versions like Ensemble Empirical Mode Decomposition (EEMD) and Improved Complete Ensemble Empirical Mode Decomposition with Adaptive Noise (ICEEMDAN), are employed to effectively extract useful information from these power signals. Traditional EMD and EEMD methods can suffer from large errors and mode mixing. The ICEEMDAN method is used to decompose the energy storage smoothing power P_{ES} [24], following these steps:

(1) Add i sets of white noise to the total energy storage power P_{ES}, constructing the sequence $P_i = P_{ES} + \varepsilon 1(w(i))$. The first set of residues $R1 = \varepsilon 1 n(Pi)$ is obtained, representing the coefficient multiplied when adding the Gaussian white noise's first IMF component $f1(w(i))$.

(2) Calculate the first mode component $imf1 = P_{ES} - R1$ Continue adding white noise and use local mean decomposition to compute the k-th set of residues $Rk = N(Rk - 1 + \varepsilon k - 1f(\text{wi}))$, and the k-th mode component: $imfk = Rk - 1 - Rk$. Repeat the above steps until the EMD decomposition is complete, ultimately obtaining all mode components imf and the corresponding residual. Perform high and low-frequency reconstruction on the decomposition results for adaptive power allocation. For the total hybrid energy storage power P_{ES}, the decomposed data can be represented as Eq. (19).

$$\begin{cases} P_{ba} = \sum_{i=1}^{n_1} imf_i \\ P_{sc} = \sum_{i=n_1+1}^{k_1} imf_j + r_1 \end{cases} \tag{19}$$

3.3 Improved Complete Ensemble Empirical Mode Decomposition with Adaptive Noise Model Optimized by Northern Goshawk Algorithm

The effectiveness of using ICEEMDAN to decompose fluctuation signals depends on the white noise amplitude weight Nstd and the number of noise additions NA. Nstd affects the noise intensity; if too large, it can cause mode mixing and reduce the quality of the decomposition. NA refers to the number of times white noise is added; if too many, it increases the computational cost. Therefore, the Northern Goshawk Optimization (NGO) algorithm is used to optimize the combination of Nstd and NA parameters, to find the optimal parameters based on the signal characteristics and complexity.

3.4 Optimization Process

In the first phase of the NGO algorithm, the primary objective is global search, aimed at enhancing the algorithm's global exploration capability. During this phase, the northern goshawk simulates randomly selecting prey in the search space and quickly attacking. This process can be described using the following mathematical formulas is Eqs. (20)–(22).

In this study, the climatic data of Ordos City in Inner Mongolia, published on the Greenwich website is taken as an example for step by step calculation and analysis, as illustrated in Fig. 4. These climatic data are input into a real-time simulation model and transformed into the output ratio of wind and solar power.

$$P_i = X_k,\ i = 1, 2, \cdots, N,\ k = 1, 2, \cdots, i-1, i+1, \cdots, N \tag{20}$$

$$X_{i,j}^{new,P1} = \begin{cases} \chi_{i,j} + r\left(P_{i,j} - I_{i,j}\right), F_{pi} < F_i \\ \chi_{i,j} + r\left(X_{i,j} - P_{i,j}\right), F_{pi} < F_i \end{cases} \tag{21}$$

$$X_i = \begin{cases} X_{i,j}^{new,P1}, F_i^{new,P1} < F_i \\ X_i, F_i^{new,P1} \geq F_i \end{cases} \tag{22}$$

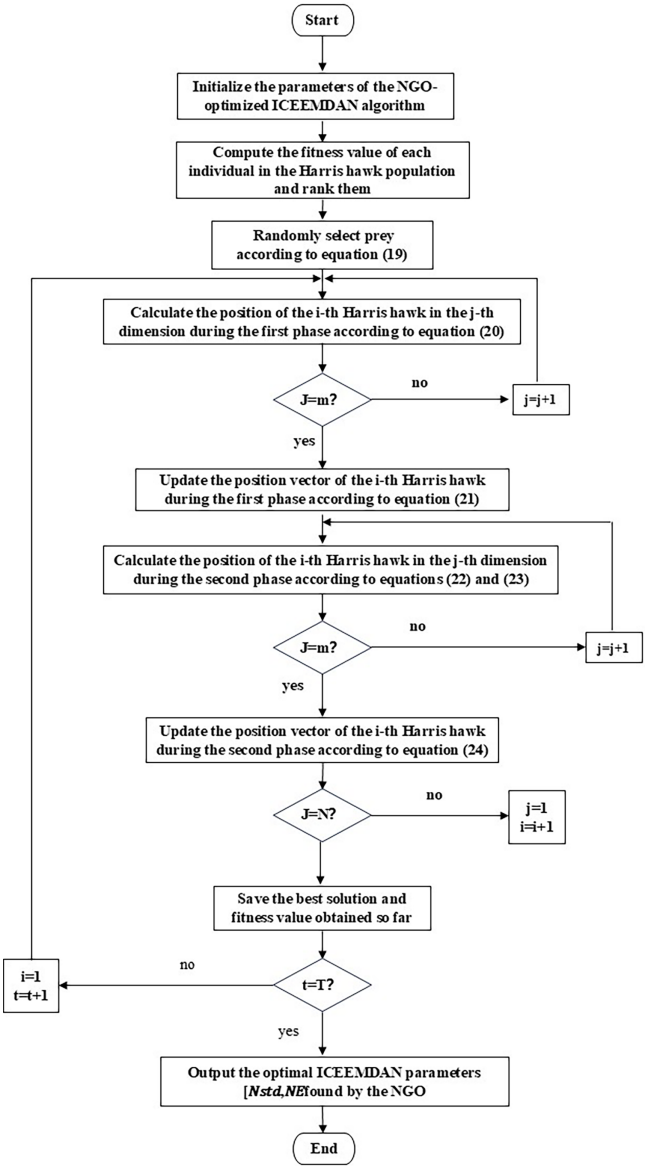

Figure 4: NGO optimization ICEEMDAN flow chart

In the second phase of the NGO algorithm, the behavior of the prey escaping after an attack and the rapid chase by the northern goshawk is simulated. The key objective in this phase is to enhance the local exploration capability of the algorithm, enabling it to meticulously search and optimize the area around the

current solutions to approach a position closer to the global optimum. R represents the attack radius of the northern goshawk. Eqs. (23)–(25) is the mathematical description of the second phase.

$$X_{i,j}^{new,P2} = X_{i,j} + R(2r-1)X_{i,j} \tag{23}$$

$$R = 0.02\left(1 - \frac{t}{T}\right) \tag{24}$$

$$X_i = \begin{cases} X_i^{new,P2}, F_i^{new,P2} < F_i \\ X_i, F_i^{new,P2} \geq F_i \end{cases} \tag{25}$$

In the equation: t and T denote the current iteration number and the maximum number of iterations, respectively; $X_i^{new,P2}$ represents the new position of the i-th Northern Goshawk; $X_{i,j}^{new,P2}$ denotes the new position of the i-th Northern Goshawk in the second stage; $F_i^{new,P2}$ is the objective function value of the i-th Northern Goshawk after the second-stage update. The detailed optimization procedure is illustrated in Fig. 4.

When using NGO to optimize ICEEMDAN parameters, selecting energy entropy as the fitness function is effective, especially for handling the randomness in hybrid energy storage power signals. Energy entropy measures the complexity of the signal by calculating the entropy based on energy distribution, describing the system's uncertainty. By minimizing energy entropy, noise and non-essential information can be effectively removed while retaining the main features.

If an intrinsic mode function (IMF) component of the signal has a low energy proportion and few characteristic information, the energy entropy increases; conversely, IMF components with more key characteristic information will have a higher energy proportion, resulting in relatively lower energy entropy.

The energy entropy Hp of the signal is calculated by evaluating the energy distribution of each component in the signal. This concept is particularly important when dealing with the mode components obtained by ICEEMDAN. The specific calculation method is Eq. (26).

$$\begin{cases} E_i = \sum_{i=1}^{k} u_i(t)^2 \\ P_i = \dfrac{E_i}{E} \\ H_p = -\sum_{i=1}^{k} P_i \log_2 P_i \end{cases} \tag{26}$$

The flowchart for optimizing ICEEMDAN parameters using NGO is shown in Fig. 3. By simulating the hunting process of northern goshawks and using energy entropy as the fitness function, the fitness of each goshawk is calculated. The iterative updates continue until the termination conditions are met. The $X_i^{new,P2}$ that minimizes the objective function $F_i^{new,P2}$ represents the optimal ICEEMDAN parameters [Nstd, NA]. This ultimately achieves the goal of NGO optimizing ICEEMDAN.

4 Case Analysis

4.1 Data Foundation

Based on the actual wind power data from a region in Inner Mongolia, China, in 2021, we conduct an analysis before applying MPC to smooth wind power fluctuations. Using the K-means clustering algorithm, we cluster the wind power data for an entire year from a wind farm with an installed capacity of 100 MW, identifying eight typical daily wind power output scenarios. The number of days corresponding to each scenario is shown in Table 1.

Table 1: Days of different scenarios

Scenario	Total number of days	Probability
1	67	0.18
2	55	0.15
3	36	0.10
4	43	0.12
5	15	0.04
6	54	0.15
7	51	0.14
8	44	0.12

When using the traditional K-means algorithm to cluster wind power output data, a major issue is that the cluster centers can be distorted by extreme data points. Extreme wind power output data may cause the cluster centers to inaccurately reflect the characteristics of the majority of the data, thus affecting the representativeness and practicality of the clustering results.

In this study, for each cluster scenario, we first calculate the cumulative fluctuation of wind power output for all the days included in the cluster to quantify the degree of daily wind power output variation. We then sort the cumulative fluctuations for all the days from highest to lowest. Finally, we select the day corresponding to the median in the sorted fluctuation list as the typical day for that cluster scenario. This method ensures that the typical day of each cluster scenario more accurately reflects the general characteristics of wind power output for that scenario, without being distorted by extreme data points. This not only improves the accuracy of the analysis but also makes subsequent wind power output predictions and management decisions more reliable.

According to the Chinese national standard "Technical Regulations for Wind Farms Connected to the Power System," wind power variations need to meet the specified limits for both 1 and 10-min time scales, as shown in Table 2. PW represents the installed capacity of the wind farm. Using MATLAB, a simulation model as shown in Fig. 1 is established. The day corresponding to the median of the typical day 5 is used as the study subject. The wind power data sampling period is 1 min, and the study duration T is 24 h. The battery energy storage system is configured with a power capacity of 25 MW and an energy capacity of 38 MWh, while the supercapacitor hybrid energy storage system is configured with a power capacity of 6 MW and an energy capacity of 0.6 MWh, based on the total life cycle cost minimization method proposed in reference [25].

Table 2: Wind power grid-connected power change standard

Wind farm installed capacity/MW	10 min maximum volatility	1 min maximum volatility
Less than 30	10	3
30–150	$P_w/3$	$P_w/10$
Greater than 150	50	15

4.2 Simulation Considering Energy Storage System Output and SOC Self-Recovery Control

Based on the above parameters and relevant indicators, the following three MPC methods can be employed for power smoothing of the hybrid energy storage system and control of the wind power grid

connection: Method 1: Optimize for the minimum output of the energy storage system and SOC balance; Method 2: Optimize in real-time considering wind power smoothing effects and SOC balance; Method 3: The optimization method proposed in this paper, dynamically optimizing for the minimum output of the energy storage system, SOC balance, and wind power smoothing effects. The parameters are set as follows: a = 0.3, b = 0.83, c = 0.3, d = 0.7, the allowed maximum grid fluctuation rate is 2%, the initial SOC values for both the battery and supercapacitor are 0.5, and the SOC upper and lower limits are 0.9 and 0.1.

Comparison of Grid-Connected Power and Fluctuation Frequency

(1) Comparison of Original Wind Power Grid Connection and Smoothed Power Figs. 5–7 show the grid-connected power, fluctuation frequency, and energy storage system output for the three control methods, respectively.

As shown in Fig. 5, by comparing the original wind power PW with the results of the three different methods, it can be seen that all three methods effectively manage the grid-connected wind power, significantly reducing output fluctuations. According to the comparison in Fig. 6a,b, the fluctuation rate of the smoothed grid-connected wind power is controlled within 2% for all three methods.

When considering the smoothing effect alone, Method 1 performs the best, with about 80% of its fluctuation rates below 0.2%. The proposed Method 3 is the second best, with about 45% of its fluctuation rates below 0.2%. Method 2 performs the worst, with less than 35% of its fluctuation rates below 0.2%, and most fluctuation rates between 0.2% and 2%.

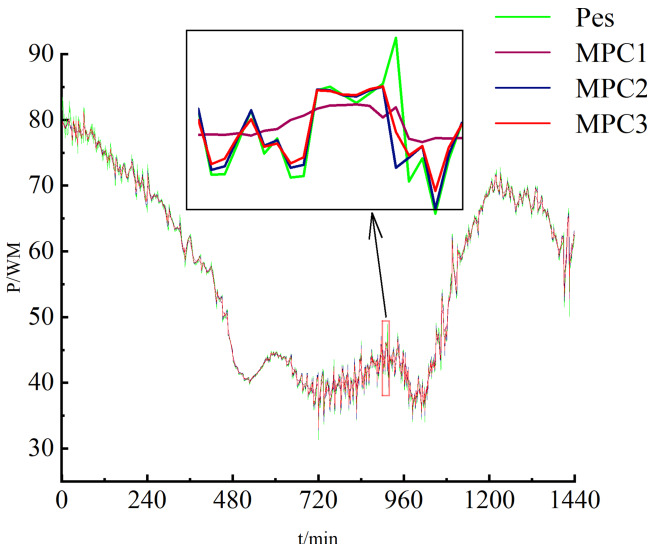

Figure 5: Grid power comparison

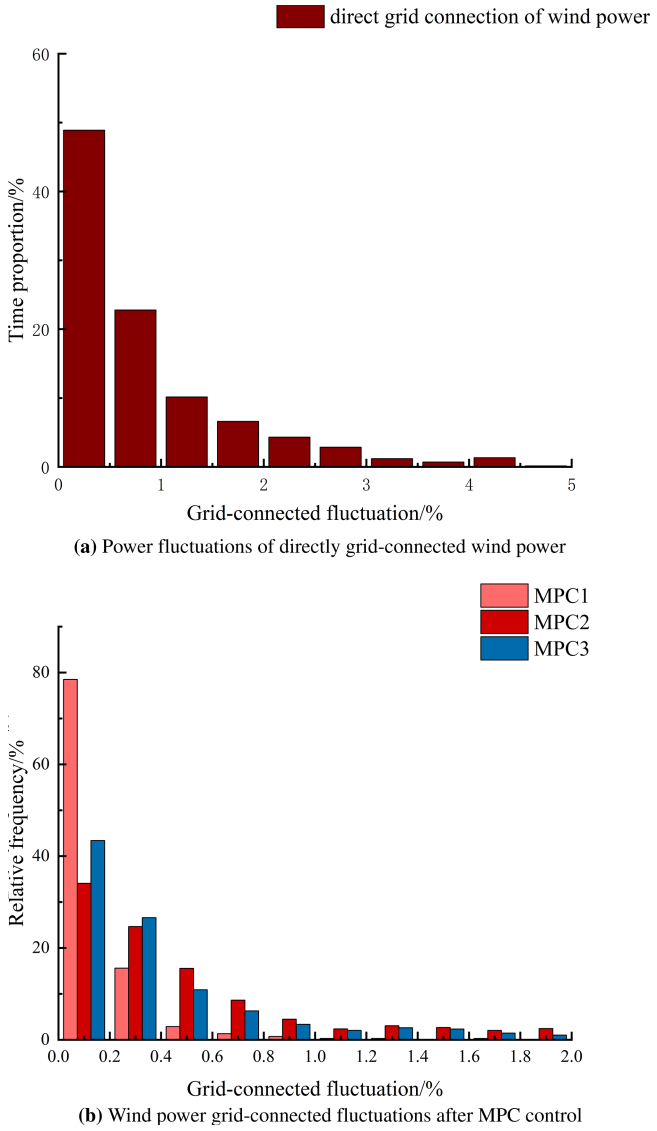

(a) Power fluctuations of directly grid-connected wind power

(b) Wind power grid-connected fluctuations after MPC control

Figure 6: Grid-connected power fluctuation rate scatter comparison diagram

According to Fig. 7, although the proposed method does not achieve as good a smoothing effect as Method 1, it significantly reduces the output of the energy storage system, making it slightly lower than Method 2. This enhances system stability and economic efficiency. The comparison shows that while Method 1 performs best in power smoothing, it may overly rely on the energy storage system, potentially leading to excessive system load and affecting long-term stability. Method 2, although less effective in smoothing, has some advantages in minimizing the output of the energy storage system.

The proposed Method 3, while considering both power smoothing effects and the output of the energy storage system, also maintains SOC balance, showing good overall performance. Particularly in terms of improving system stability and economic efficiency, Method 3 demonstrates significant advantages. Therefore, Method 3 not only provides a good power smoothing effect but also exhibits higher reliability and economic efficiency in the long-term operation and maintenance of the energy storage system.

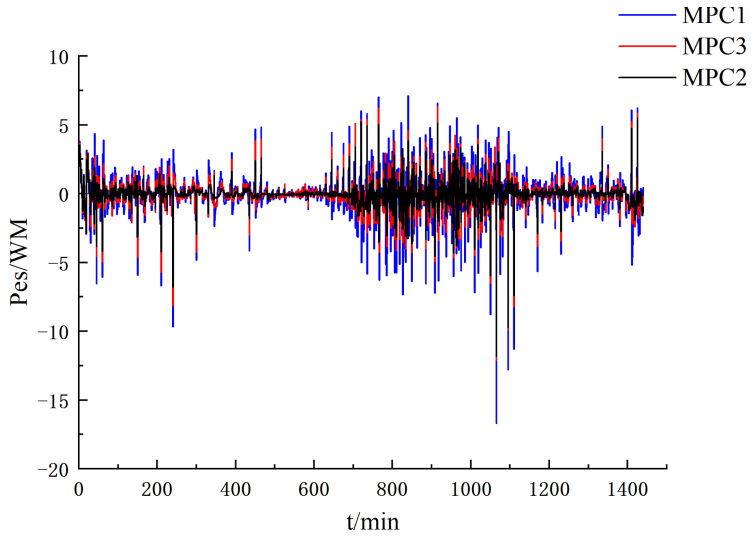

Figure 7: Energy storage system output comparison diagram

(2) Comparison of Hybrid Energy Storage SOC Changes

When controlling the energy storage system to smooth wind power, it is insufficient to use only the grid-connected wind power fluctuation rate as the standard for evaluating the control strategy. The operational state of the energy storage system not only affects the lifespan and overall economic efficiency of the storage components but also impacts the long-term smoothing effect of wind power.

Fig. 8 shows the SOC changes of the HESS under the three control strategies, and Fig. 9 shows the corresponding SOC distribution. These charts provide in-depth insights into the behavior of the energy storage system under different control strategies, helping to evaluate the feasibility and efficiency of each strategy in practical applications.

By analyzing SOC changes and distributions, we can identify the strengths and weaknesses of each strategy in the operation of the energy storage system. This analysis provides a basis for optimizing energy storage system control strategies.

Analysis from Figs. 8 and 9 show significant differences in the SOC performance of the HESS under the three control strategies. In Method 1, the energy storage system operates within the safe charge-discharge range of [0.3, 0.7] for 75% of the time, effectively maintaining stable wind power operation while keeping the SOC balanced as much as possible. Method 2 focuses on maintaining SOC balance and minimizing the output of the energy storage system. The results show that the SOC stays within the optimized charge-discharge range of [0.4, 0.6] for 85% of the time, and within the safe range of [0.3, 0.7] for over 95% of the time. Adjustments to the energy storage system for smoothing fluctuations are made only during severe wind power fluctuations. The strategy in Method 3 keeps the SOC within the [0.3, 0.7] range for approximately 82% of the time, falling between Method 1 and Method 2. The comparison shows that Method 2 performs best in maintaining SOC balance and system stability, while Method 3 has certain advantages in balancing smoothing effects and operational efficiency of the system.

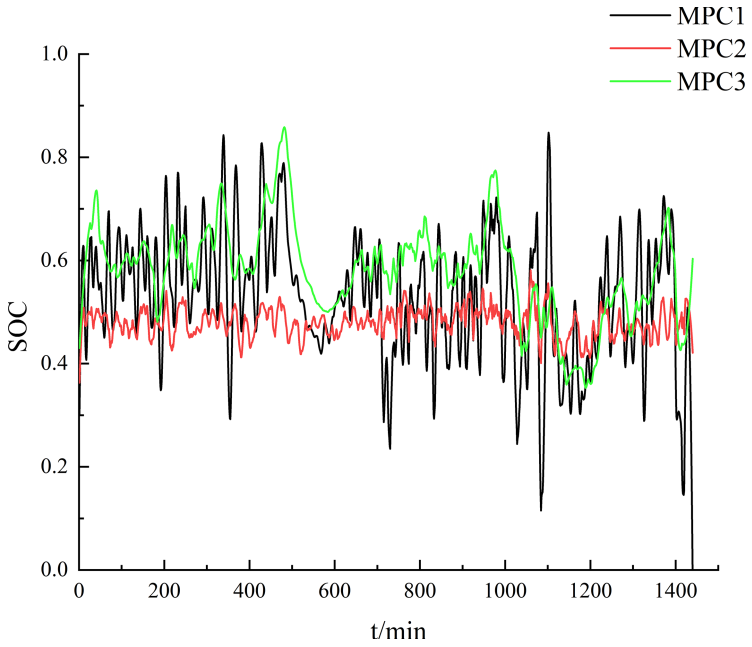

Figure 8: Comparison of hybrid energy storage SOC changes

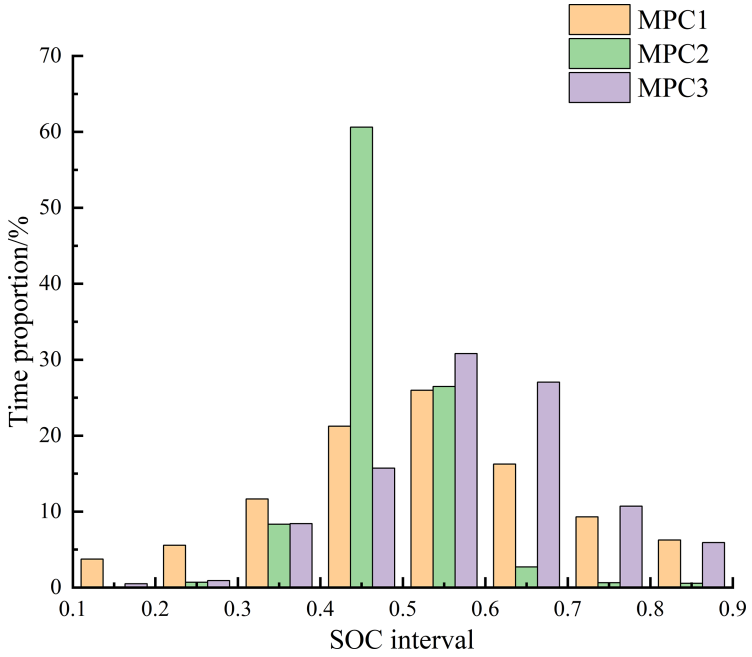

Figure 9: Comparison of SOC distribution of hybrid energy storage

4.3 Secondary Power Allocation of Hybrid Energy Storage System Based on NGO-Optimized ICEEMDAN

Using MPC, the HESS achieves the initial target power for smoothing wind power fluctuations, meeting the preliminary requirements for managing wind power variability. However, to fully utilize the advantages of lithium batteries and supercapacitors within the HESS, further coordination in power allocation is necessary. In this process, the large capacity of lithium batteries should be leveraged to smooth large power fluctuations,

while the rapid response and frequent charge-discharge capabilities of supercapacitors should be used to handle high-frequency power loads. This approach can reduce the number of charge-discharge cycles for lithium batteries, thereby extending their lifespan.

This section adopts the NGO-ICEEMDAN method to decompose the target power, determining the power allocation for lithium batteries and supercapacitors through high-frequency and low-frequency reconstruction. To demonstrate the relative advantages of NGO-ICEEMDAN in HESS power allocation, we compare the power changes and SOC changes of supercapacitors and lithium batteries before and after NGO optimization as evaluation metrics.

First, ICEEMDAN is used to decompose the reference power of the hybrid energy storage system, resulting in nine intrinsic mode functions (IMFs) from high to low frequency and one residual. Through Hilbert transformation, the instantaneous frequency-time curves for each mode function can be obtained (here, only IMF5–IMF9 and the residual curves are listed).

As shown in Fig. 10, there is mode mixing between adjacent IMF5 and IMF6 components, making it difficult to find an appropriate frequency to separate the high-frequency and low-frequency parts. Consequently, the battery will still bear part of the high-frequency power fluctuations, affecting its cycle life.

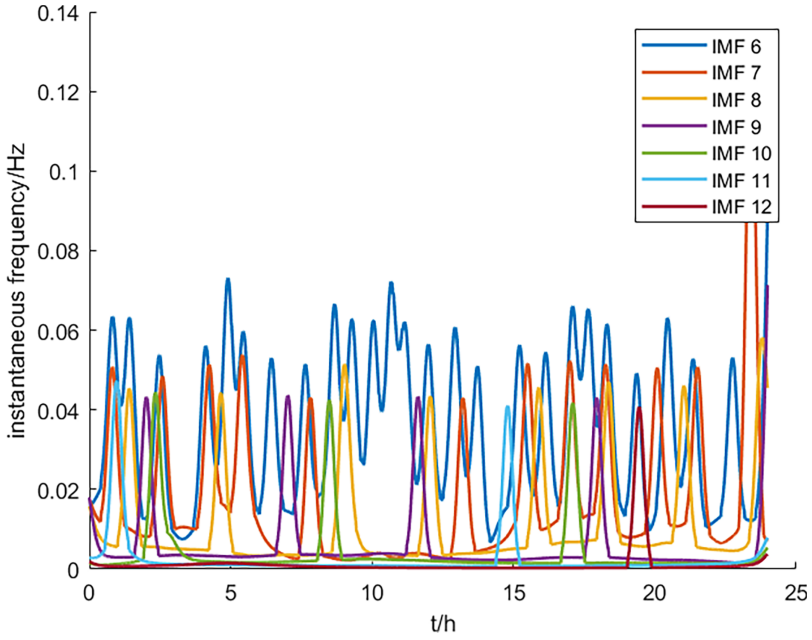

Figure 10: Curve of instantaneous frequency-time of some ICEEMDAN's IMF

Next, the NGO-ICEEMDAN method is used to decompose the reference power of the hybrid energy storage system. As shown in Fig. 11, this results in 12 IMFs from high to low frequency and one residual. By applying Hilbert transformation to these 12 mode functions, the instantaneous frequency-time curves for each mode can be obtained (here, only IMF5–IMF11 are listed).

As shown in Fig. 12, there is almost no mode mixing between the curves of IMF5 and IMF6 throughout the entire period. Therefore, the mode functions at IMF5 and higher frequencies are reconstructed to form the reference power for the supercapacitor, while IMF6 and the remaining lower frequency components are reconstructed to form the reference power for the lithium battery.

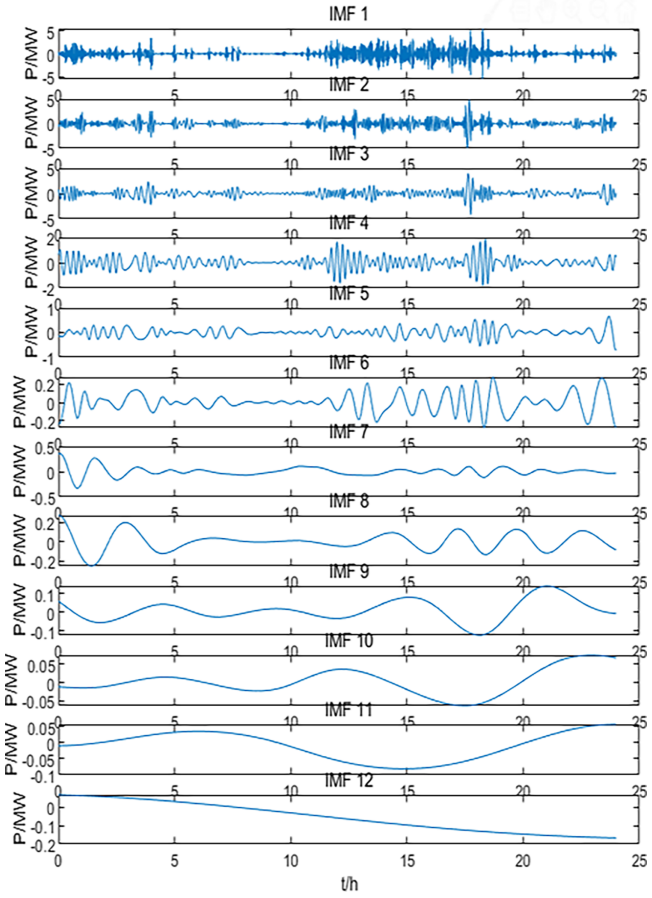

Figure 11: Curve of IMF and remnant decomposed by NGO-ICEEMDAN

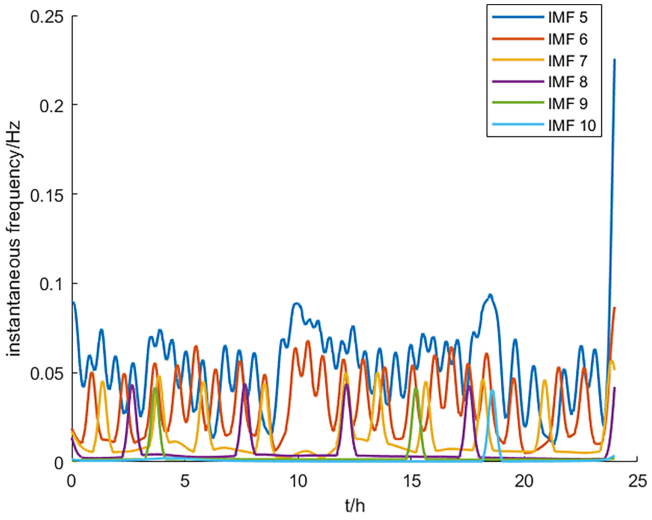

Figure 12: Curve of instantaneous frequency-time of some NGO-ICEEMDAN's IMF

The NGO-ICEEMDAN method proposed in this paper is used for MPC rolling optimization, and the resulting hybrid energy storage target power allocation is shown in Fig. 13. Fig. 13a shows the comparison of

battery smoothing power between the two decomposition methods, and Fig. 13b shows the comparison of supercapacitor smoothing power.

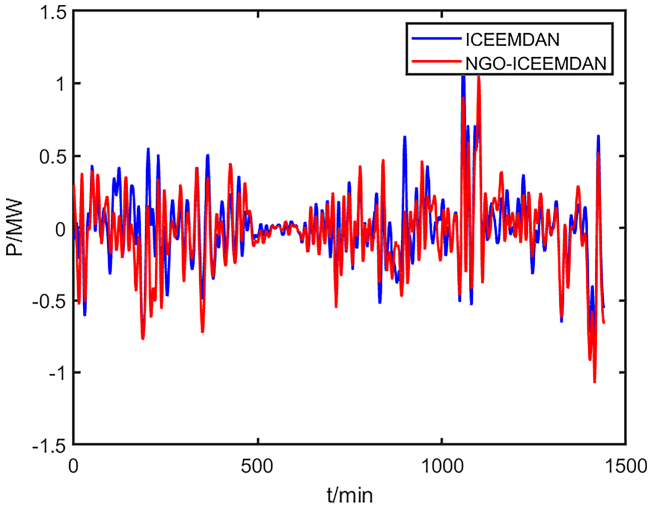

(a) Battery power distribution.

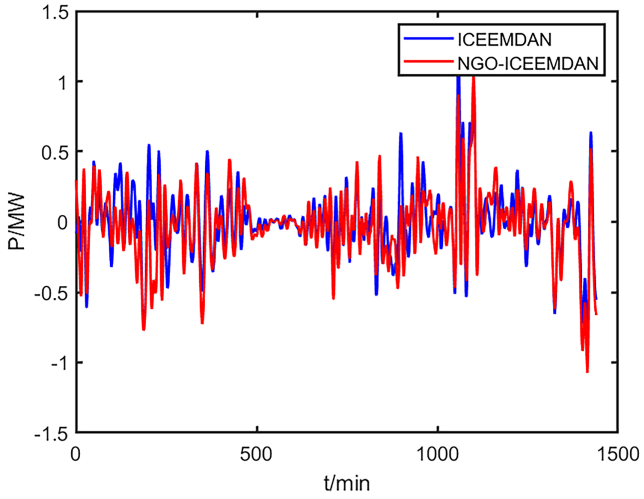

(b) Supercapacitor power distribution.

Figure 13: Power distribution of HESS before and after optimization

Compared to the traditional method, the battery's power variation is more stable. Throughout the wind power smoothing process, the battery handles large power fluctuations, while the supercapacitor manages frequent small power fluctuations, fully utilizing the performance advantages of both lithium batteries and supercapacitors. As can be seen in Fig. 13a, the low-frequency component fluctuations of the battery obtained from the NGO-optimized ICEEMDAN decomposition are significantly lower than those from the non-optimized ICEEMDAN method.

In summary, the method proposed in this paper can adjust the power allocation of the energy storage system according to different power fluctuation demands, thereby more effectively smoothing wind power fluctuations.

5 Conclusion

It should be noted that this study still has certain limitations. The simulation analysis is based solely on wind power data from the Inner Mongolia region, which limits data diversity and may affect the generalizability of the results to other regions with different renewable characteristics. In addition, the absence of hardware-in-the-loop and experimental testing restricts the evaluation of the proposed strategy's real-world feasibility and control performance. Despite these limitations, the study demonstrates that stand-alone energy storage stations, functioning as "temporal and spatial regulators" of power systems, play a vital role in modern grids. The hybrid energy storage system composed of lithium iron phosphate batteries and supercapacitors effectively smooths wind power fluctuations and enhances system stability. In the short term, it can deliver economic value through arbitrage and ancillary services, while in the long term, it supports the development of highly resilient grid architectures with renewable penetration exceeding 80%. Based on the above analysis, the main research findings of this study are as follows:

(1) This paper designs an MPC control strategy that considers both SOC recovery and minimum output of the energy storage system. The simulation results show that the proposed control method is superior to Method 2 in smoothing wind power fluctuations, with the duration of fluctuation rates less than 0.2% being approximately 10% longer than Method 2. The minimum output condition of the energy storage system is better than Method 1, with the SOC operating within the [0.3, 0.7] range for about 7% longer than Method 1. The analysis results indicate that the proposed control strategy not only effectively smooths wind power fluctuations but also optimizes the SOC operating range and minimizes the output of the energy storage system, thereby reducing the wear and tear on the storage system.

(2) The NGO-ICEEMDAN method is used to decompose the hybrid energy storage power, finding the optimal white noise amplitude weight Nstd and the number of noise additions NA. Before optimization, the combination of Nstd and NA was [0.1, 10], and after optimization, it was [0.0507, 7]. Through high-frequency and low-frequency reconstruction, reasonable power allocation between the battery and supercapacitor is achieved. The simulation results show that using NGO-ICEEMDAN makes the power curve of the battery more stable and fully utilizes the fast response characteristics of the supercapacitor, thereby extending the lifespan of the energy storage equipment.

This paper studies the smoothing of wind power fluctuations and the coordinated and stable operation of the hybrid energy storage system in a wind-storage combined system. However, there are still some unresolved issues or areas that require further research, such as optimizing the capacity configuration of the hybrid energy storage system to further leverage the performance advantages of supercapacitors and increasing experimental validation when conditions permit. In addition, the current study mainly focuses on a relatively small-scale system under idealized operating conditions, which may not fully capture the complexity of large-scale wind farms or wind–solar hybrid systems. The scalability and adaptability of the proposed strategy under varying environmental conditions, diverse grid connection scenarios, and different renewable penetration levels require further investigation. Moreover, the influence of economic constraints, system reliability, and long-term degradation of hybrid energy storage components should be comprehensively evaluated in future work.

Acknowledgement: The author would like to thank the New Energy Storage Department of Ordos Energy Research Institute of Peking University for its important support in providing RT-LAB and other simulation tools, and the Key Laboratory of Wind Energy and Solar Energy of Inner Mongolia University of Technology for providing the necessary test site for this paper.

Funding Statement: The funding for this paper was provided by the Science and Technology Project of Inner Mongolia Electric Power (Group) Corporation Limited, 2025 (Project No. 2025-3-1).

Author Contributions: Jiguang Wu: funding acquisition, methodology, projection administration, resources, writing—review and editing; Qing Zhi: writing—original draft, software, data curation, validation and conceptualization; Jin Guan: writing—original draft, investigation and validation; Ruopeng Zhang: writing—review and editing, validation and data curation; Lixia Wu: validation, supervision, investigation and resources; Shuhui Zhang: formal analysis, investigation, validation and supervision; Caifeng Wen: supervision, writing—review and editing. All authors reviewed the results and approved the final version of the manuscript.

Availability of Data and Materials: Some of the experimental data and optimization data used in this study have been uploaded to the database, accessible at: https://doi.org/10.5281/zenodo.17141282 (accessed on 20 November 2025).

Ethics Approval: Not applicable.

Conflicts of Interest: The authors declare no conflicts of interest to report regarding the present study.

References

1. Byers C, Botterud A. Additional capacity value from synergy of variable renewable energy and energy storage. IEEE Trans Sustain Energy. 2020;11(2):1106–9. doi:10.1109/tste.2019.2940421.
2. Ren G, Wang W, Wan J, Hong F, Yang K, Yu D. Investigating the impacts of spatial-temporal variation features of air density on assessing wind power generation and its fluctuation in China. Sci China Technol Sci. 2023;66(6):1797–814. doi:10.1007/s11431-022-2248-4.
3. Amaro Pinazo M, Romeral Martinez JL. Intermittent power control in wind turbines integrated into a hybrid energy storage system based on a new state-of-charge management algorithm. J Energy Storage. 2022;54:105223. doi:10.1016/j.est.2022.105223.
4. Qiu Z, Zhang W, Lu S, Li C, Wang J, Meng K, et al. Charging-rate-based battery energy storage system in wind farm and battery storage cooperation bidding problem. CSEE J Power Energy Syst. 2022;3:659–68. doi:10.17775/CSEEJPES.2021.00230.
5. Wan C, Qian W, Zhao C, Song Y, Yang G. Probabilistic forecasting based sizing and control of hybrid energy storage for wind power smoothing. IEEE Trans Sustain Energy. 2021;12(4):1841–52. doi:10.1109/tste.2021.3068043.
6. Liao Y, Yang C, Bai J, He Q, Wang H, Chen H, et al. Insights into the cycling stability of manganese-based zinc-ion batteries: from energy storage mechanisms to capacity fluctuation and optimization strategies. Chem Sci. 2024;15(20):7441–73. doi:10.1039/d4sc00510d.
7. Guo T, Liu Y, Zhao J, Zhu Y, Liu J. A dynamic wavelet-based robust wind power smoothing approach using hybrid energy storage system. Int J Electr Power Energy Syst. 2020;116:105579. doi:10.1016/j.ijepes.2019.105579.
8. Puchalapalli S, Singh B, Das S. Grid-interactive smooth transition control of wind-solar-DG based microgrid at unpredictable weather conditions. IEEE Trans Ind Applicat. 2024;60(1):1519–29. doi:10.1109/tia.2023.3322396.
9. Gao X, Fu L. SOC optimization based energy management strategy for hybrid energy storage system in vessel integrated power system. IEEE Access. 2020;8:54611–9. doi:10.1109/access.2020.2981545.
10. Eydi M, Alishahi M, Zarif M. A novel output power determination and power distribution of hybrid energy storage system for wind turbine power smoothing. IET Electr Power Appl. 2022;16(12):1559–75. doi:10.1049/elp2.12240.
11. Neshat M, Nezhad MM, Abbasnejad E, Mirjalili S, Tjernberg LB, Astiaso Garcia D, et al. A deep learning-based evolutionary model for short-term wind speed forecasting: a case study of the Lillgrund offshore wind farm. Energy Convers Manage. 2021;236:114002. doi:10.1016/j.enconman.2021.114002.
12. Ding M, Wu J. A novel control strategy of hybrid energy storage system for wind power smoothing. Electr Power Compon Syst. 2017;45(12):1265–74. doi:10.1080/15325008.2017.1346004.
13. Yuan T, Guo J, Yang Z, Feng Y, Wang J. Optimal configuration of electro-hydrogen hybrid energy storage capacity for smoothing wind power fluctuations. Proc CSEE. 2024;44(4):1397–406. doi:10.13334/j.0258-8013.pcsee.222572.
14. Wang X, Zhou J, Qin B, Guo L. Coordinated power smoothing control strategy of multi-wind turbines and energy storage systems in wind farm based on MADRL. IEEE Trans Sustain Energy. 2024;15(1):368–80. doi:10.1109/tste.2023.3287871.

15. Oh B, Kim S, Lee D. Wind power scenario synthesis with smoothing effect through spectral decomposition and its application to flexible resource adequacy. IEEE Trans Sustain Energy. 2023;14(2):777–89. doi:10.1109/tste.2022.3225272.
16. Majidi Nezhad M, Heydari A, Neshat M, Keynia F, Piras G, Garcia DA. A mediterranean sea offshore wind classification using MERRA-2 and machine learning models. Renew Energy. 2022;190:156–66. doi:10.1016/j.renene.2022.03.110.
17. Wang L, Wang Y, Liu C, Yang D, Chen Z. A power distribution strategy for hybrid energy storage system using adaptive model predictive control. IEEE Trans Power Electron. 2020;35(6):5897–906. doi:10.1109/tpel.2019.2953050.
18. Pahasa J, Ngamroo I. Two-stage optimization based on SOC control of SMES installed in hybrid wind/PV system for stabilizing voltage and power fluctuations. IEEE Trans Appl Supercond. 2021;31(8):1–5. doi:10.1109/tasc.2021.3089119.
19. Ma L, Xie LR, Ye L, Lu P, Wang KF. Wind power fluctuation smoothing strategy based on hybrid energy storage two-layer planning model. Power Syst Technol. 2022;46(3):1016–29. (In Chinese). doi:10.13335/j.1000-3673.pst.2021.0569.
20. Lin L, Cao Y, Kong X, Lin Y, Jia Y, Zhang Z. Hybrid energy storage system control and capacity allocation considering battery state of charge self-recovery and capacity attenuation in wind farm. J Energy Storage. 2024;75:109693. doi:10.1016/j.est.2023.109693.
21. Cao M, Xu Q, Qin X, Cai J. Battery energy storage sizing based on a model predictive control strategy with operational constraints to smooth the wind power. Int J Electr Power Energy Syst. 2020;115:105471. doi:10.1016/j.ijepes.2019.105471.
22. Yao B, Cai Y, Liu W, Wang Y, Chen X, Liao Q, et al. State-of-charge estimation for lithium-ion batteries based on modified unscented Kalman filter using improved parameter identification. Int J Electrochem Sci. 2024;19(5):100574. doi:10.1016/j.ijoes.2024.100574.
23. Li J, Sun H, Zhao W, Liang C, Liang Z, Yuan X. Power distribution strategy of wind power hybrid energy storage system based on variational mode decomposition and multi-fuzzy control. J Shanghai Jiao Tong Univ. 2025;59(10):1498. doi:10.3390/en17225650.
24. Liang Y, Lin Y, Lu Q. Forecasting gold price using a novel hybrid model with ICEEMDAN and LSTM-CNN-CBAM. Expert Syst Appl. 2022;206:117847. doi:10.1016/j.eswa.2022.117847.
25. Lin L, Lin YL, Tan HD, Jia YQ, Kong XY, Cao YP. Control of hybrid energy storage for smoothing wind power fluctuations considering SOC self-recovery. Trans China Electrotech Soc. 2024;39(3):658–71. (In Chinese). doi:10.19595/j.cnki.1000-6753.tces.221976.